Journal of ELECTRONIC MATERIALS, Vol. 47, No. 8, 2018
https://doi.org/10.1007/s11664-018-6395-2

TOPICAL COLLECTION: 18TH INTERNATIONAL CONFERENCE ON II-VI COMPOUNDS

Growth and Characterization of Type I Quantum Wells Based on ZnCdSe/ZnTe Type II Heterostructures Confined within ZnSe Barriers

JUAN CARLOS BANTHÍ-BARCENAS,[1] FRANTISEK SUTARA,[2] and ISAAC HERNÁNDEZ-CALDERÓN [1,2,3]

1.—DNyN Program, Center for Research and Advanced Studies (Cinvestav), Ave. IPN 2508, 07360 Mexico City, Mexico. 2.—Physics Department, Center for Research and Advanced Studies (Cinvestav), Ave. IPN 2508, 07360 Mexico City, Mexico. 3.—e-mail: Isaac.Hernandez@fis.cinvestav.mx

We present our results related to the growth, photoluminescence characterization and modelling of a quantum well (QW) involving a type II heterostructure, $Zn_{1-x}Cd_xSe/ZnTe/Zn_{1-x}Cd_xSe$, confined within ZnSe barriers with a type I band alignment. We show that this type of hybrid QWs may be employed for the elaboration of $Zn_{1-x}Cd_xSe/ZnSe/GaAs$ based red emitters without exceeding a Cd content around 42%. The design of the ZnSe/$Zn_{1-x}Cd_xSe/ZnTe/Zn_{1-x}Cd_xSe$/ZnSe QW was based on calculations employing the transfer matrix method under the effective mass, envelope function approximation. The QW was epitaxially grown at 275°C on a semi-insulating GaAs (001) substrate by a combination of molecular beam epitaxy for the ZnSe barriers, submonolayer pulsed beam epitaxy for the ZnCdSe layers of the QW and atomic layer epitaxy for the central ZnTe QW layer. A heterostructure with a central region of 2 ZnTe monolayers surrounded at each side by seven monolayers of $Zn_{1-x}Cd_xSe$, with $x \sim 0.41$, presented a room temperature exitonic deep red emission with a peak at 1.829 eV.

Key words: II–VI semiconductor quantum wells, type II interfaces, epitaxy, ZnSe, ZnCdSe, ZnTe

INTRODUCTION

In the typical quantum well (QW) type I structures the electrons and holes are confined in the same spatial regions. However, there are cases where the interfaces of two semiconductors align in such a way that only the valence band (VB) or only the conduction band (CB) of one of the materials is situated within the bandgap of the other, then we have type II alignment of the bands. In such case, the charge carriers are spatially separated; only one type of carrier is confined in a quantum well, while, in the same region, a barrier is formed for the other type of carrier. This characteristic of type II heterostructures makes them very attractive in basic research and for application in semiconductor devices. Several type II heterostructures of II-VI semiconductors have been epitaxially elaborated since the mid 1980s.[1,2] In the past few years, diverse type II heterostructures based on II-VI compounds have shown quite interesting properties, as mentioned in the following examples. Type II ZnTe/ZnSe quantum dots present fast decay emission properties with holes confined within the ZnTe quantum dots (QDs) and electrons in ZnSe around the dots.[3] Strong Aharonov-Bohm effects persisting at temperatures up to 180 K have been observed in type-II ZnTe/ZnSe QDs.[4] Submonolayer ZnTe/ZnCdSe QDs have been suggested as an intermediate material for solar cells.[5] More recently, ZnSe/CdS/ZnS QDs have been used as fluorescent labels for biomedical studies.[6]

(Received January 22, 2018; accepted May 18, 2018; published online June 8, 2018)

$Zn_{1-x}Cd_xSe$/ZnSe interfaces present a type I band alignment for any x.[7] On the other hand, the ZnSe/ZnTe and CdSe/ZnTe interfaces present a type II band alignment,[8] therefore, $Zn_{1-x}Cd_xSe$/ZnTe interfaces for any $0 \le x \le 1$ are also type II. We will take advantage of the distinct types of band alignment of those interfaces to elaborate QW heterostructures with optical transitions with lower energy than any of the band gaps of the constituent semiconductors. In this work, we present the epitaxial growth and photoluminescence (PL) characterization of a QW based on a type II $Zn_{1-x}Cd_xSe$/ZnTe/$Zn_{1-x}Cd_xSe$ active region within ZnSe barriers that result in type I confinement of the active region. The design of the heterostructure is based on our previously reported model calculations,[9] which are based on the effective mass, envelope function approximations and the transfer matrix method. The effects of strain induced by the lattice mismatch of the layers were considered in all the calculations.

We show that this type of hybrid heterostructure, besides its interesting fundamental properties, allows the elaboration of systems based on $Zn_{1-x}Cd_xSe$ with emission in the red spectral range at relatively low Cd contents. The ultra-thin ZnTe layer allows the use of ZnCdSe alloys with $x \sim 0.4$; without this ultra-thin layer insertion is not possible to obtain red emission with $x \le 0.60$. The epitaxial growth of ZnCdSe films with such a high amount of Cd is very difficult due to the large lattice mismatch with the GaAs substrates and in most of the cases we obtain low quality films with a high density of dislocations, stacking faults and other defects, as well as composition fluctuations. Of course, red emitters have been in production for many years, mainly based on III-VI compounds. Red emitters have been also produced with II-VI semiconductors employing $Zn_{1-x}Cd_xSe$/ZnCdMgSe QWs on lattice matched InP substrates,[10] however, in our case, we are interested in heterostructures grown on GaAs substrates, considering advantageous their low cost and mechanical robustness. The hybrid type I–type II QW design presented in this work makes possible to extend the spectral range of II–VI heterostructures grown on GaAs substrates with active regions based on ZnCdSe/ZnSe QWs. It allows coverage of the full red-blue spectrum with relatively simple to prepare QW heterostructures in comparison with, for example, the QW heterostructures grown on InP substrates that usually require the employment of quaternary alloys and, therefore, a more complex growth.

HYBRID TYPE I–TYPE II QUANTUM WELL DESIGN

Figure 1 shows the band structure and electronic levels of the type II $Zn_{1-x}Cd_xSe$/ZnTe/$Zn_{1-x}Cd_xSe$ active region with type I confinement induced by the ZnSe barriers.[9] Some values in this figure were obtained after the measurement of the excitonic emission of the heterostructure, as will be explained later. It is important to note that the entire system represents a single QW with a non-conventional stepped potential. We want to point out that this heterostructure was designed considering the constraints of its epitaxial growth with high crystalline quality by taking into account the lattice mismatch of the constituent semiconductor layers. To avoid the formation of misfit dislocations, that would affect the performance of the system, the QW was intended to grow pseudomorphic to the ZnSe barriers. Considering the lattice mismatch, up to 2.98% between $Zn_{1-x}Cd_xSe$ ($x \le 0.41$) and ZnSe, and the lattice mismatch of 7.69% between ZnTe and ZnSe (in this pseudomorphic structure the lattice constant parallel to the interfaces of all layers is that of ZnSe), few monolayers (MLs) thick ZnCdSe layers and a central ZnTe region with maximum thickness of 2 MLs (around 0.66 nm) are required. The selected thicknesses of the QW layers are shown in Fig. 2. The bulk values of band gap energies were taken from Ref. 11, however, the band gap energies of the pseudomorphic QW layers are affected by compressive strains of -2.88% and -7.14% for $Zn_{0.59}Cd_{0.41}Se$ and ZnTe, respectively, resulting in band gap values higher than those of the bulk materials (2.307 eV and 2.390 eV for $Zn_{0.59}Cd_{0.41}Se$ and ZnTe, respectively), these stress modified values are shown in Fig. 1.

EXPERIMENTAL DETAILS

The QW structure was epitaxially grown on a semi-insulating GaAs (001) substrate at ~ 275°C in a Riber 32P system with a base pressure of 7×10^{-12} kPa. The GaAs (001) substrate was deoxidized by thermal annealing around 560°C in ultra-high vacuum. $A \sim 500$ nm ZnSe buffer layer was then grown by molecular beam epitaxy (MBE). The

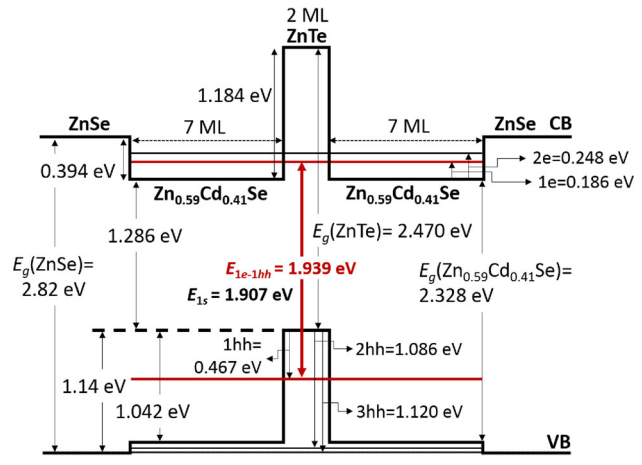

Fig. 1. Diagram of a QW with a type II $Zn_{1-x}Cd_xSe$/ZnTe/$Zn_{1-x}Cd_xSe$ active region subjected to a type I confinement induced by the ZnSe barriers. The band gaps of ZnTe and $Zn_{1-x}Cd_xSe$ correspond to the strained films. $E_{1e\text{-}1hh}$ is the fundamental transition of the QW and E_{1s} refers to the excitonic transition.

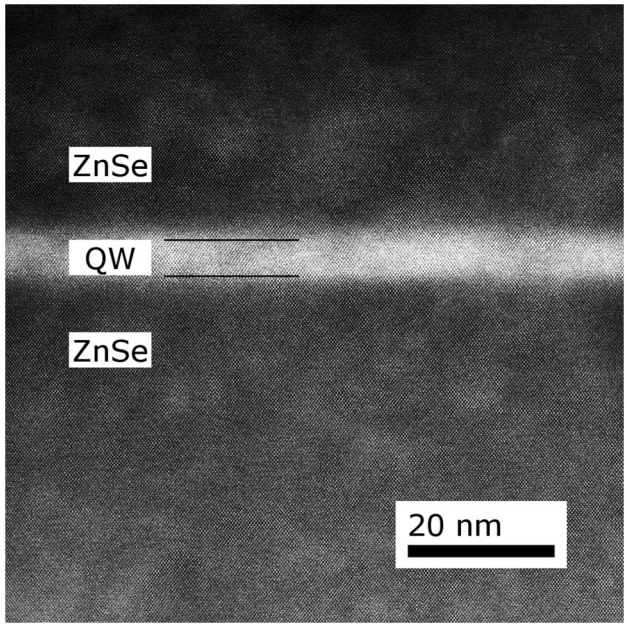

Fig. 2. Dark field STEM micrograph of the hybrid QW taken at 200 keV. The QW presents a uniform thickness and well defined interfaces. The horizontal black lines represent an expected QW thickness of around 4.9 nm.

QW active region, consisting of a central 2 MLs thick ZnTe layer surrounded at each side by 7 MLs of ZnCdSe, was grown in a layer-by-layer mode by combination of submonolayer pulsed beam epitaxy[12] for the $Zn_{1-x}Cd_xSe$ layers of the QW and atomic layer epitaxy for the ZnTe layer. The QW structure was then finished with $\sim$ 70 nm thick ZnSe capping layer grown by MBE. The structural quality of the layers was monitored during the growth by reflection high energy electron diffraction (RHEED) employing a 30 keV electron beam.

Scanning transmission electron microscopy (STEM) images of the structure were obtained with a JEOL ARM200F microscope, equipped with a spherical aberration corrector, at 200 keV. PL experiments at low (19 K) and room temperature (RT) were performed employing a typical setup with a 0.5 m Spex monochromator, a closed circuit He refrigerator and a lock-in detection. The 442 nm HeCd laser line was used for the optical excitation of the sample.

RESULTS AND DISCUSSION

Figure 2 presents a low magnification dark field STEM image of the sample taken at 200 keV. We can observe well-defined and flat QW/barrier interfaces. Two horizontal black lines represent the expected strained QW thickness of around 4.9 nm obtained from the calculations. We observe a quite good agreement with the experiment considering the nature of the epitaxial growth procedure based on the self-regulated layer-by-layer deposition methods employed for the growth of the QW layers.

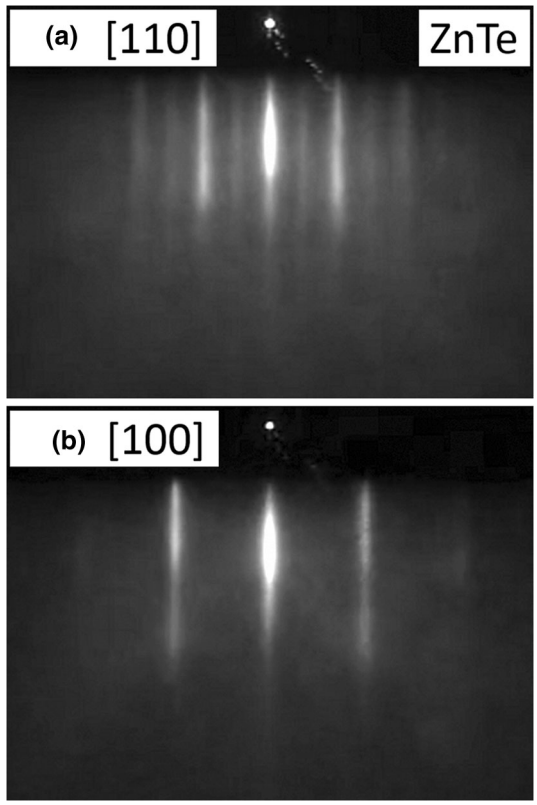

Fig. 3. RHEED patterns of the Te terminated surface of the ZnTe layer along the (a) [110] and (b) [100] azimuths taken after finishing the growth of the 2 MLs of ZnTe. The well-defined streaks of the (2 $\times$ 1) surface reconstruction are a clear indication of its 2-D growth.

A slightly larger apparent QW thickness could be attributed to the diffusely scattered background, projection of atomic steps in the beam direction and to damage produced by the Ga ion bombardment during the lamella preparation. Although the ultra-thin central ZnTe layer cannot be resolved due to very low Z-contrast between Cd and Te containing layers, we can exclude alloying of QW layers and/or formation of 3-D structures, as supported by the fact that the optical properties of the heterostructure are pretty well as expected from the model calculations assuming flat abrupt interfaces. Furthermore, the layer-by-layer growth of the ZnTe ultra-thin film and its high crystalline surface quality was demonstrated by the streaky RHEED pattern exhibiting a clear (2 $\times$ 1) surface reconstruction for the Te terminated surface, see Fig. 3. A systematic high-resolution STEM study is underway and more detailed information with the chemical identification of the 2 ML ZnTe central region will be published elsewhere. Figure 4a shows the PL spectra at 19 K and 300 K of the heterostructure taken with the 442 nm line of a HeCd laser, the excitation power was around 14 mW, and the emission was intense even at 300 K. At 300 K a deep red excitonic emission (1.829 eV, 677.9 nm) was observed. To our knowledge, this is the lowest energy emission

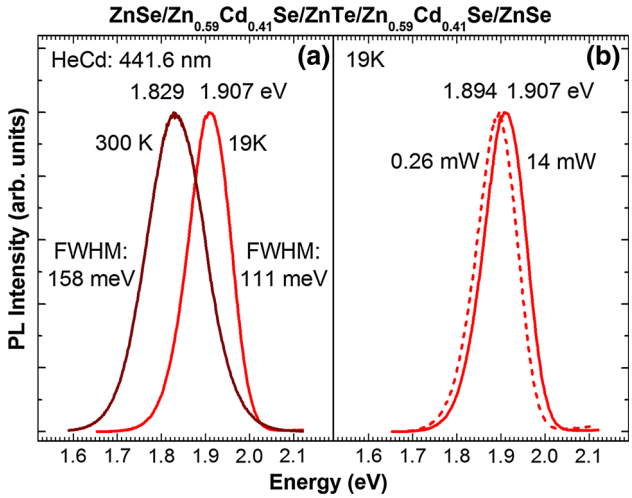

Fig. 4. PL spectra of the hybrid QW showing (a) red luminescence at 19 K and RT. The full width at half maximum (FWHM) values are indicated for each spectrum. The RT excitonic emission at 1.829 eV is of a deep red color. (b) The solid line spectra were acquired at 14 mW excitation power, the dashed line spectrum at 0.26 mW. All spectra are normalized to the same height (Color figure online).

produced by a $Zn_{1-x}Cd_xSe$ based QW grown on GaAs (001). As expected, a shift to higher energies is observed at low temperature. The peaks are of Gaussian shape and relatively broad compared to the emissions in the yellow[13] and blue-green regions,[14] we attribute this to the inhomogeneous broadening produced by the various layers that constitute the QW. The dashed line in Fig. 4b represents the PL spectrum at 19 K acquired with a lower excitation power of 0.26 mW. The observed 13 meV red shift with respect to the PL spectrum excited with 14 mW illustrates the excitation power dependence of the excitonic emission peak energy, a behavior typical for type II structures, suggesting that the charge carriers in the QW are, to a certain extent, spatially separated.

Employing the 19 K experimental value of the excitonic emission (1.907 eV), the band gap of ZnSe, and the band gap value of the strained ZnTe (2.470 eV, instead of the bulk value of 2.39 eV), the best fit of the calculations to the experimental excitonic transition indicated a Cd content of 41.3% in the $Zn_{1-x}Cd_xSe$ alloy and a valence band offset (VBO) of 1.14 eV between ZnSe and ZnTe. Once those values were determined, the rest of the values of the electronic levels and the band offsets of $Zn_{1-x}Cd_xSe$/ZnTe that appear in Fig. 2 were calculated. The calculated excitonic emission indicated in Fig. 2, E_{1s} = 1.907 eV, is obtained subtracting the exciton binding energy of 32 meV to the fundamental 1e − 1hh transition (hh is the heavy hole level). The exciton binding energy was calculated employing the fractional-dimensional space model.[15,16] Just to appreciate the role of the 2 ML ZnTe central region with type II alignment with respect to the adjacent $Zn_{0.59}Cd_{0.41}Se$ layers, note that the excitonic emission of a QW with the same total thickness (16 MLs), but made only of $Zn_{0.59}Cd_{0.41}Se$, would be of 2.413 eV (513.7 nm), a quite green emission.

SUMMARY AND CONCLUSIONS

We have produced a II–VI QW epitaxial heterostructure based on a type II $Zn_{0.59}Cd_{0.41}Se$ (7 MLs)/ZnTe (2 MLs)/$Zn_{0.59}Cd_{0.41}Se$ (7 MLs) QW active region subjected to type I confinement induced by ZnSe barriers. The elaboration of the QW was performed after the design of the heterostructure employing the effective mass, envelope function approximations and the transfer matrix method. The effects of strain produced by the lattice mismatch of the layers were considered. From the combined results of the experiments and calculations, a valence band offset of 1.14 eV between ZnSe and ZnTe was determined. The active region of the QW (a total of 16 MLs) was grown in a layer-by-layer mode. The energy of the excitonic emission at 19 K was 1.907 eV. At RT the intense emission shifted to 1.829 eV (677.9 nm), a deep red color. To our knowledge, this is the lowest emission energy produced with a QW based on the $Zn_{1-x}Cd_xSe$/ZnSe/GaAs heterostructure. The presented heterostructure exhibited a high emission intensity similar to the conventional type I ZnCdSe/ZnSe QW systems, nevertheless, the insertion of the ultrathin ZnTe layer with type II band alignment in the central region of the QW provided some characteristics typical for type II systems, e.g., the excitation power dependence of the excitonic emission energy, and allowed reaching significantly lower excitonic emission energy, in comparison with a similar structure without this layer.

ACKNOWLEDGEMENTS

We acknowledge the partial support of Conacyt-Mexico. JCBB thanks Conacyt-Mexico for a Ph. D. scholarship. We thank the Advanced Laboratory of Electron Nanoscopy (LANE) for the STEM images, particularly Daniel Bahena and Alvaro Angeles.

REFERENCES

1. T. Takeda, T. Kurosu, M. Lida, and T. Yao, *Surf. Sci.* 174, 548 (1986).
2. H. Luo, N. Samarth, F.C. Zhang, A. Pareek, M. Dobrowolska, and J.K. Furdyna, *Appl. Phys. Lett.* 58, 1783 (1991).
3. R. Andre, R. Najjar, L. Besombes, C. Bougerol, S. Tatarenko, and H. Mariette, *Phys. Status Solidi C* 6, 857 (2009).
4. I. Sellers, V. Whiteside, I. Kuskovsky, A. Govorov, and B. McCombe, *Phys. Rev. Lett.* 100, 136405 (2008).
5. S. Dhomkar, U. Manna, L. Peng, R. Moug, I.C. Noyan, M.C. Tamargo, and I.L. Kuskovsky, *Sol. Energy Mater. Sol. Cells* 117, 604 (2013).
6. S. Wang, J.J. Li, Y. Lv, R. Wu, M. Xing, H. Shen, H. Wang, L.S. Li, and X. Chen, *Nanoscale Res. Lett.* 12, 380 (2017).
7. E.T. Yu, M.C. Phillips, J.O. McCaldin, and T.C. McGill, *J. Vac. Sci. Technol. B* 9, 2233 (1991).
8. Y. Rajakarunanayake, R.H. Miles, G.Y. Wu, and T.C. McGill, *J. Vac. Sci. Technol. B* 6, 1354 (1988).

9. J.C. Banthí-Barcenas, F. Sutara, and I. Hernández-Calderón, *AIP Conf. Proc.* 1934, 03001 (2018).
10. M.C. Tamargo, W. Lin, S.P. Guo, Y. Guo, Y. Luo, and Y.C. Chen, *J. Cryst. Growth* 214, 1058 (2000).
11. I. Hernández-Calderón, Optical properties and electronic structure of wide band gap II–VI semiconductors.*II–VI Semiconductor Materials and their Applications*, ed. M.C. Tamargo (New York: Taylor and Francis, 2002), pp. 113–170.
12. I. Hernández-Calderón, Epitaxial growth of thin films and quantum structures of II–VI visible-bandgap semiconductors.*Molecular Beam Epitaxy: From Research to Mass Production*, ed. M. Henini (Oxford: Elsevier, 2013), pp. 310–346.
13. G. Villa-Martínez, J.C. Banthí-Barcenas, D. Bahena, F. Sutara, and I. Hernández-Calderón, *J. Vac. Sci. Technol. B* 34, 041225 (2016).
14. I. Hernández-Calderón, M. García-Vázquez, L.M. Hernández-Ramírez, and M.A. Vidal, *J. Vac. Sci. Technol. B* 29, 03C137 (2011).
15. X.-F. He, *Phys. Rev. B* 43, 2064 (1991).
16. H. Mathieu, P. Lefebvre, and P. Christol, *Phys. Rev. B* 46, 4092 (1992).